206. Cationic Rh^I Complexes of Azulenes and Their Catalytic Activity on the Formation of Heptalene-1,2-dicarboxylates from Dimethyl Acetylenedicarboxylate and Azulenes

by **Andreas Johannes Rippert**[1]), **Anthony Linden**, and **Hans-Jürgen Hansen***

Organisch-chemisches Institut der Universität, Winterthurerstr. 190, CH-8057 Zürich

Dedicated to *Duilio Arigoni* on the occasion of his 65th birthday

(2.VIII.93)

$[Rh^I(\eta^5\text{-azulene})(cod)]^+BF_4^-$ complexes **3a–g** (cod = (*Z,Z*)-cycloocta-1,5-diene) have been synthesized by reaction of $[Rh^I(cod)]^+BF_4^-$ in THF with the corresponding azulenes **1a–g** (*Table 1*). The structure of $[Rh^I(cod)(\eta^5\text{-guaiazulene})]^+BF_4^-$ (**3a**) has been determined by X-ray diffraction analysis (*Fig. 1* and *2*). The Rh-atom is oriented above the five-membered ring of the azulene with almost equal Rh–C distances to all five C-atoms of the ring. The (*Z,Z*)-cycloocta-1,5-diene ring occurs in two enantiomorphic distorted ($C_{2v} \rightarrow C_2$) tub conformations in the crystals (*Fig. 3*). In $CDCl_3$ solution, the cod ligand in the complexes **3** shows a dynamic behavior on the ^{1}H-NMR time scale which is best explained by rotation of the cod ligand relative to the azulene ligands around an imaginary cod–Rh–azulene axis. The new complexes **3** catalyze the formation of heptalene-1,2-dicarboxylates **2** from dimethyl acetylenedicarboxylate (ADM) and the corresponding azulenes **1** just as effectively as $[RuH_2(PPh_3)_4]$ and the analogous $[RhH(PPh_3)_4]$ complex in MeCN solution (*Table 3*). On grounds of simplicity, **3** can be generated *in situ*, when $[RhCl(cod)]_2$ is applied as catalyst (*Table 3*).

Introduction. – Recently, we have shown that the yield of heptalene-1,2-dicarboxylates **2** formed from azulenes **1** and dimethyl acetylenedicarboxylate (ADM) in apolar solvents at temperatures > 180° can be improved substantially, when the reaction is carried out in the presence of a catalytic amount of $[RuH_2(PPh_3)_4]$ in a polar aprotic solvent such as MeCN (*Scheme 1*) [1]. The reaction of 1-(*tert*-butyl)-4,6,8-trimethylazulene with ADM in the presence of the catalyst yielded, even at 25°, dimethyl 11-(*tert*-butyl)-2,4,6-trimethyltricyclo[6.2.2.$0^{1,7}$]dodeca-2,4,6,9,11-pentaene-9,10-dicarboxylate, which represents the *Diels-Alder*-type adduct of ADM and the five-membered ring of the azulene. Since this type of adduct is also the established primary intermediate in the

Scheme 1

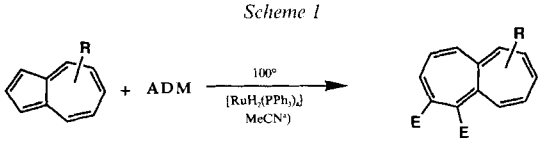

1 **2** (20–100%)

[a]) 2 mol-% of the catalyst in 0.1M solution of **1** in the presence of 3 mol-equiv. of ADM. E = $COOCH_3$.

[1]) Part of planned Ph. D. thesis of *A. J. R.*, University of Zurich.

purely thermal reaction of azulenes with ADM in apolar solvents (*cf.* [2] [3]), we postulated that, in the catalytic variant of the reaction, a Ru^0 complex carrying an ADM ligand at the d^8 center is formed at the five-membered ring of the azulene in the crucial step leading to the tricyclic intermediate (*cf.* Scheme 5 in [1]).

To the best of our knowledge, transition-metal complexes of azulenes are not very well known. It has been reported by *Schrock* and *Osborn* [4] that $[Rh(nbd)]^+$ ions (nbd = norbornadiene), generated in THF, react with azulene at 25° to form a deep-red η^5-complex with the electron-rich five-membered ring of azulene. At room temperature, this complex shows a rapid exchange between free and coordinated azulene. In this paper, we report on a general synthesis of Rh^I complexes of azulenes and (*Z*,*Z*)-cycloocta-1,5-diene (cod) and describe their structural and spectroscopic as well as catalytic properties.

Results and Discussions. – The $[Rh^I(\eta^5\text{-azulene})(cod)]^+BF_4^-$ salts **3** shown in *Table 1* were all obtained by the same procedure. $[Rh(cod)]^+BF_4^-$ was generated in THF solution from $[Rh(cod)Cl]_2$ and $AgBF_4$. After removal of AgCl, the corresponding azulenes **1** were added. The complex salts **3**, which could be recrystallized from acetone, were precipitated as deep-red microcrystals from the THF solution by addition of Et_2O. The complex salts **3** were stable in air as well as in solution, in solvents such as acetone, CH_2Cl_2, $CHCl_3$, or benzene. However, they easily lost their azulene ligand in coordinating solvents such as alcohols (MeOH, EtOH) or MeCN. It was also observed that the greater the number of Me substituents, that are located on the five-membered ring of azulenes **1**, the more stable are these complexes, even in coordinating solvents. For example, whereas the deep-red color of **3b** (*Entry 2* in *Table 1*) in EtOH at room temperature changed completely within 1 h into the blue color of the free azulene **1b**, the red color of **3g** (*Entry 7* in *Table 1*) in EtOH was still observable after 24 h, and ligand exchange had occurred only to *ca.* 50% (UV/VIS evidence). *Fig. 1* shows the structure of **3a** (*Entry 1* in *Table 1*) as derived from a low-temperature X-ray diffraction analysis of racemic crystals which had been obtained by recrystallization from acetone solution. The Rh-atom is, indeed, located above the five-membered ring of the azulene skeleton of **1a**, as has already been postulated by *Schrock* and *Osborn* [4] for the corresponding $[Rh^I(\eta^5\text{-azulene})(\eta^4\text{-nbd})]^+BF_4^-$ complex on the basis of ^{1}H-NMR measurements. The Rh–C distances for the C-atoms of the

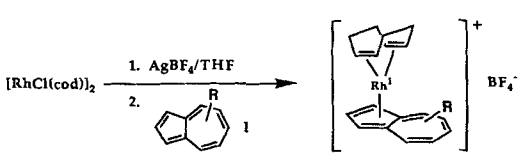

Table 1.
Formation of $[Rh^I(\eta^5\text{-azulene})(cod)]^+BF_4^-$ **(3)**

Entry	R: Position Nr.	Azulene Nr.	Complex [%]	*Yield* [°C]	*M.p.*
1	Me: 1,4, i-Pr: 7	**1a**	**3a**	91	229.7–230.2
2	Me: 4,6,8	**1b**	**3b**	81	190.8–192.1
3	Me: 2,4,6,8	**1c**	**3c**	86	249.9–250.8
4	Me: 4,6,8, E: 2	**1d**	**3d**	68	210.8–212.0
5	Me: 1,3, *t*-Bu: 6	**1e**	**3e**	82	179.8–180.6
6	Me: 1,3,4,8	**1f**	**3f**	87	200.9–201.8
7	Me: 1,2,3,4,6,8	**1g**	**3g**	89	210.5–211.6

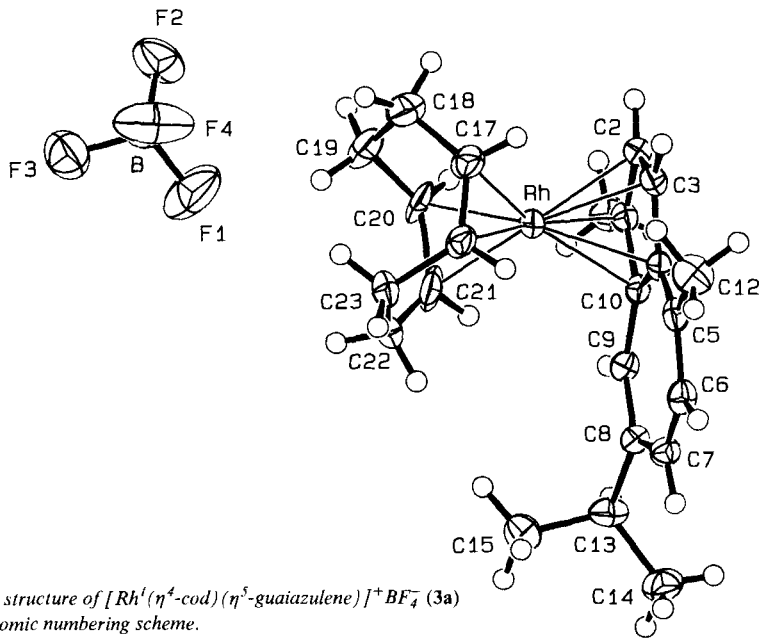

Fig. 1. *Crystal structure of* $[Rh^{I}(\eta^{4}\text{-cod})(\eta^{5}\text{-guaiazulene})]^{+}BF_4^{-}$ (**3a**) *showing the atomic numbering scheme.*

five-membered ring are nearly all the same within the experimental error (227(1) pm excluding Rh–C(3), which is slightly shorter; see *Exper. Part*) and are of a similar magnitude to those observed in other [Rh^{I}(cp)] complexes (see *e.g.* [5]; cp = cyclopentadienide). The C=C bonds of the cod ligand are oriented nearly parallel to the longitudinal axis of **1a**, *i.e.* nearly parallel to the plane of the azulene. The tub conformation of the cod ligand is distorted from C_{2v} to C_2, as has been observed for a number of other [Rh^{I}(cod)] complexes (*cf.* [5–7] and lit. cited therein) and other transition-metal complexes with cod (*cf.* [8] [9] and lit. cited therein). The refinement of the crystal diffraction data of **3a** revealed that the cod ligand is disordered in the crystal with two distinct, equally occupied orientations with respect to the azulene ring (*Fig. 2, a* and *b*). The first orientation, which is represented in *Fig. 2, a* (and also in *Fig. 1*), shows that the Me–C(1) at the five-membered ring of the azulene and the olefinic H-atoms at C(20) and C(21) of the cod ligand are in a somewhat staggered arrangement with respect to an imaginary axis passing through the middle of the cod and five-membered rings and the Rh-atom, whereas H–C(3) of the azulene and the olefinic H-atom at C(17) of the cod ligand describe an eclipsed arrangement. In the second orientation (*Fig. 2, b*), the cod ligand is rotated (*ca.* 30°) around the imaginary cod–Rh–guaiazulene axis, so that H–C(16A) and H–C(17A) of the cod ligand are in a staggered position with respect to H–C(3) of the azulene, and, in turn, H–C(2A) of the cod ligand and Me–C(1) of the azulene are placed in an eclipsed arrangement. However, of greater interest is the fact that the C_2-distorted cod ligand possesses an (*M*)-conformation in the first orientation and a (*P*)-conformation in the second one, *i.e.* the two cod conformations are almost mirror images which means that the crystals are diastereomorphic mixtures. *Fig. 3* shows the

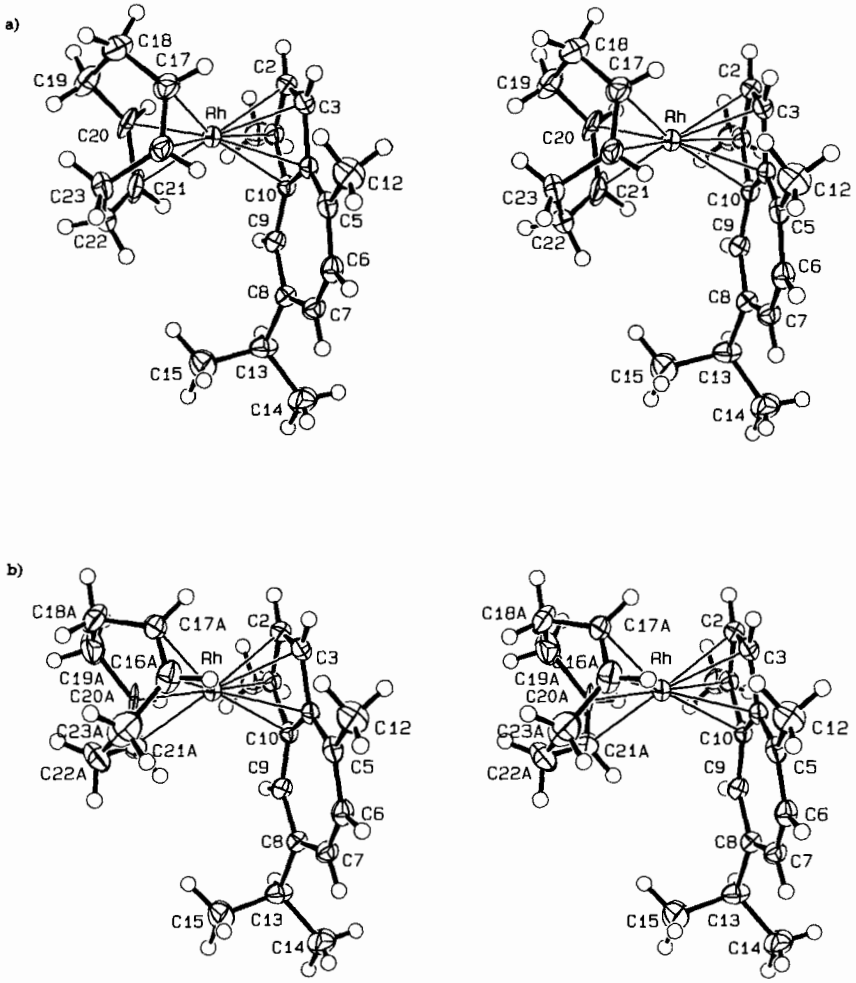

Fig. 2. *Stereoscopic projection of the X-ray structure of* $[Rh^{I}(cod)(\eta^{5}\text{-guaiazulene})]^{+}BF_4^-$ (**3a**) *with the two resolved and refined orientations* (*a* and *b*) *of the cod ligand* (the BF_4^- ions have been omitted for the sake of clarity)

enantiomorphic orientations of the cod ligand in a mirror-image arrangement (the left-hand fragment has been rotated on the page to enhance the visual comparison) with the corresponding torsion angles around the $C(sp^3)$–$C(sp^3)$ bond.

Table 2 contains some characteristic VIS and ^{1}H-NMR spectroscopic data of the new complexes **3**. The VIS spectra (CH_2Cl_2) of **3a–g** are quite typical in that the weak azulene absorption bands, responsible for the blue color of the free azulenes, have completely vanished in the coordinated azulenes, and have been replaced by a new broad absorption band of medium intensity ($\log \varepsilon = 3.8$) in the range of 505 to 525 nm. This new band is responsible for the deep-red color of complexes **3** in the crystals as well as in solution. The UV absorption bands of **3** (see *Exper. Part*) are similar to those of the free ligands **1**.

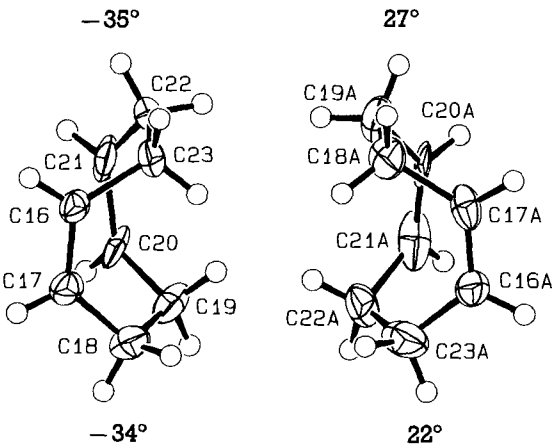

Fig. 3. *Projection of the two mirror image C_2 conformations of the cod ligand found in the crystals of [Rh^I(cod)(η^5-guaiazulene)]$^+BF_4^-$* (**3a**) (the angles indicate the observed C_4 torsional angles along the C(sp^3)–C(sp^3) bonds)

Table 2. *Some Characteristic Spectroscopic Data of [Rh^I(η^5-azulene)(cod)]$^+BF_4^-$* (**3**)[a])

Complex Nr.	VIS[b]) [nm] (log ε)	^{1}H-NMR[c]) [ppm]				^2J(H–C(2),^{103}Rh) [Hz]
		R–C(1)	R–C(3)	R–C(2)	Olef. H of cod	
3a	517.1 (3.73)	2.23 (*s*) (2.82)	6.25 (*d*) (7.22)	7.20 (*t*) (7.61)	5.01 4.34	1.74
3b	505.6 (3.78)	6.23 (*d*)		7.20 (*td*)	4.70	1.88
3c	508.2 (3.83)	6.22 (*s*)		2.76 (br. *s*)	4.68	[d])
3d	523.0 (3.84)	6.43 (*s*)		[4.09 (*s*)][e])	4.78	–
3e	524.9 (3.77)	2.22 (*s*) (2.61)		7.07 (*d*) (7.48)	4.55	1.67
3f	522.6 (3.82)	2.37 (*s*) (2.80)		6.93 (*d*) (7.23)	4.37	1.24
3g	516.6 (3.79)	2.33 (*s*) (2.94)		2.53 (*d*) (2.43)	4.25	[1.27][f])

[a]) *Cf. Table 1.*
[b]) In CH_2Cl_2; for UV absorption bands, see *Exper. Part.*
[c]) In $CDCl_3$ at 300 MHz. R = H or Me in the corresponding positions. In parentheses are the chemical shifts in the corresponding free azulenes **1**. For the complete set of ^{1}H-NMR data, see *Exper. Part.*
[d]) ^3J(*Me*–C(2),^{103}Rh) resulted only in a broadening of the signal of Me–C(2).
[e]) R = $COOCH_3$.
[f]) ^3J(*Me*–C(2),^{103}Rh).

A comparison of the ^{1}H-NMR shifts of the substituents at C(1)–C(3) of the five-membered ring of the azulenes (R = H or Me; *Table 2*) shows that complex formation did indeed take place at the five-membered ring (*vide supra*), and that the complexes **3** are stable in $CDCl_3$, since no line broadening is observable.

In particular, the substituents at C(1) and C(3) undergo a substantial high-field shift upon complexation. On the other hand, the change upon complexation is only moderate

for H–C(2) and even reverse for Me–C(2). These shift properties are in agreement with the fact that the HOMO of the azulenes possesses the largest orbital coefficients at C(1) and C(3), whereas a nodal plane passes through C(2) and C(8).

It is of interest to note that, in all complexes **3** carrying H–C(2), we observed ^2J(H–C(2),^{103}Rh) in the range of 1.2–1.9 Hz (*Table 2*). ^2J Values of this size have also been reported with other Rh complexes (*cf.* [10]). However, similar ^2J values were not observed with H–C(1) and/or H–C(3) (*cf.* **3b–d** in *Table 2*). An analogous effect is found for ^3J(H,^{103}Rh) which, in general, is smaller than ^2J(H,^{103}Rh)) (*cf.* [10]) and, in our case, is only observable with Me–C(2) in **3g** (and supposedly in **3c**), but not with Me–C(1,3) (see **3g** as well as **3a**, **3e**, and **3f**). In contrast to these observations, the ^{13}C-NMR spectra ($CDCl_3$) of all complexes **3** showed ^1J(^{13}C,^{103}Rh) in the order of 2.5–5.0 Hz for all five C-atoms of the five-membered ring of the azulene ligands (*cf. Exper. Part*). However, as a rule, we found that ^1J(^{13}C(2),^{103}Rh) is always larger (3.8–5.0 Hz) in comparison with the other ^1J values (2.6–4.1 Hz). The magnitude of these coupling constants fits well within the range of ^1J(^{13}C,^{103}Rh) observed for other Rh complexes (*cf.* [10]).

The chirality of complex **3a** is also evident from its ^{1}H-NMR spectrum in $CDCl_3$, since the i-Pr group appears as 2*d* at 1.414 and 1.408 ppm, *i.e.* **3a** shows signals for diastereotopic Me groups.

The signals for the cod ligand in the complexes are broad and not resolved indicating a dynamic exchange process for the H sites in the cod ligand. This exchange process can at best be explained by a relative rotation of the cod ligand around an imaginary cod–Rh–azulene axis with respect to the azulene ligand, as has been proposed for the dynamic behavior of other transition-metal cod complexes (*cf.* [9] and lit. cited therein). For such a process to occur, we have to expect (*cf. Scheme 2*) that a C_2-symmetric site

Scheme 2. *Suggested Dynamic Exchange Process of the H-Atom Sites in the cod Ligand of* **3a** (only the H-atoms at the C=C bonds are shown)

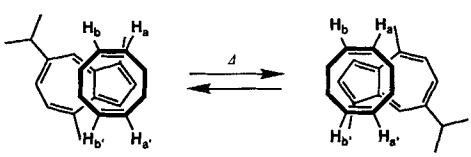

exchange must take place, *i.e.* at the C=C bonds, H_a and $H_{b'}$, as well as $H_{a'}$ and H_b, are interconverting. Indeed, all symmetrically substituted complexes **3b–g** show only one broad resonance line for the H-atoms at the C=C bonds of their cod ligand in the range of 4.3–4.7 ppm[2]). On the other hand, complex **3a**, carrying the unsymmetrically substituted guaiazulene (**1a**) ligand, exhibits two broad signals at 5.01 and 4.34 ppm for the olefinic H-atoms of the cod ligand, in agreement with the suggested exchange process (*Fig. 4*). Since irradiation of the signal from Me–C(5) causes a ^{1}H-NOE of medium intensity on the signal at 4.34 ppm and only a weak ^{1}H-NOE on the signal at 5.01 ppm, we can assign the first signal to $H_a/H_{b'}$ (*Scheme 2*; H–C(20)/H–C(16) in *Fig. 1*) and, correspondingly,

[2]) Similarly, the H-atoms on the allylic positions of the cod ligands show mainly one broad resonance signal at room temperature.

the second one to H_b/H_a (H–C(21)/H–C(17) in *Fig. 1*)[3]). The average chemical shift of the olefinic H-atoms of **3a** (4.68 ppm) corresponds very well with that of the symmetrically substituted complexes **3b** and **3c**.

The observed chemical shifts of the olefinic H-atoms of the cod ligands correlate qualitatively with the stability of the complexes **3** in coordinating solvents such as ROH, *i.e.* the greater the shielding effect, the more stable these complexes become.

Since we had postulated that the active complex in the formation of heptalene-1,2-dicarboxylates from azulenes and ADM in the presence of $[RuH_2(PPh_3)_4]$ (*Scheme*) is a Ru^0 complex (*vide supra* as well as [1] [11]), we also examined the isoelectronic $[RhH(PPh_3)_4]$ complex for its catalytic activity and found that it is nearly as active as $[RuH_2(PPh_3)_4]$ (*cf. Table 3, Entries 1* and *2*). This led us to investigate also the reactivity of complex **3a** in the presence of ADM. Indeed, when **3a** was heated with an equimolar amount of ADM in MeCN the corresponding heptalene-1,2-dicarboxylate **2a** was formed in a yield of 23.5% (*Table 3, Entry 3*). The yield of **2a** could be improved substantially, when **3a** was

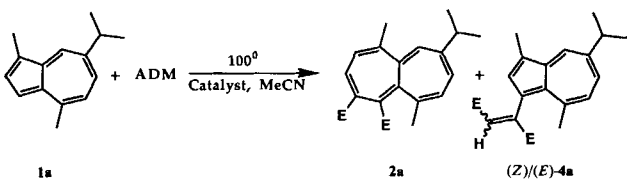

1a **2a** (*Z*)/(*E*)-**4a**

Table 3. *Catalysis of the Formation of Heptalene-1,2-dicarboxylate* **2a** *from Guaiazulene* (**1a**) *and ADM*[a])

Entry	Catalyst	ADM		Yields [%]		
		[mol-%]	[equiv.]	Heptalene **2a**	(*Z*)-**4a**	(*E*)-**4a**
1[b])	$[RuH_2(PPh_3)_4]$	2	3	80	8	8
2	$[RhH(PPh_3)_4]$	2	3	65	10.6	6.2
3	**3a**	100	1	23.5	19	9
4	**3a**	2	3	82.4	5.3	2.9
5	$[RhCl(cod)]_2/2AgBF_4$	1	3	80.2	6.4	2.7
6	$[RhCl(cod)]_2$	1	3	79.1	5.3	3.8

[a]) For details, see *Exper. Part.*
[b]) Data taken from [1].

applied in only catalytic amounts (*Table 3, Entry 4*). *Entry 5* in *Table 3* shows that the catalytically active complex (**3a** in our model case) can also be generated *in situ* in MeCN by the reaction of $[RhCl(cod)]_2$ with $AgBF_4$ in the presence of the corresponding azulene (**1a** in our model case). However, further experiments revealed that it is not necessary to generate $[Rh(cod)]^+$ ions from $[RhCl(cod)]_2$ and $AgBF_4$, since $[RhCl(cod)]_2$ itself is catalytically active in the formation of heptalene-1,2-dicarboxylates such as **2a** (*Table 3, Entry 6*). The formation of the accompanying products (*Z*)- and (*E*)-**4a**, which represent the acid-catalyzed products of azulenes and ADM (*cf.* [12] [13]), could not be suppressed completely.

[3]) At a temperature where the exchange process is slow, four signals for the olefinic H-atoms should be observable. The symmetric complex **3g** in CD_2Cl_2 at −60° shows, indeed, two broad signals at 4.20 and 4.28 ppm for the olefinic H-atoms of the cod ligand.

The experiments described above demonstrate that complexes of Ru- or Rh-azulene with coordinated ADM molecules play a key rôle in catalyzing the formation of dimethyl tricyclo[6.2.2.$0^{1,7}$]dodeca-2,4,6,9,11-pentaene-9,10-dicarboxylates, which are crucial primary intermediates in heptalene-1,2-dicarboxylate production from azulenes and ADM (*cf. Scheme 5* in [1]).

We thank Prof. *W. von Philipsborn* for discussions and his coworkers for NMR support and our microanalytical laboratory under the direction of *H. Frohofer* for elemental analyses. The financial support of this work by the *Schweizerischer Nationalfonds zur Förderung der wissenschaftlichen Forschung* is gratefully acknowledged.

Experimental Part

General. M.p. on a *Büchi* apparatus (model *FP5*). The values are not corrected. UV spectra on an *Otsuka* spectrophotometer (model *MCPD 1100*); maxima and minima (λ_{max} and λ_{min}) are given in nm (log ε). IR spectra ($CHCl_3$) on a *Perkin-Elmer* IR spectrophotometer (model *FT-IR 1600*); band positions are given in cm^{-1}. ^1H, ^{13}C-, and ^{103}Rh-NMR spectra on *Bruker* instruments (models *AC 300, AM 400*) or a *Varian* instrument (model *XL 200*).

1. *Rh^I-Azulene Complexes.* All reactions were performed under Ar in oven-dried *Schlenk* vessels. THF (*Fluka, puriss.*) was purified over a column of basic Al_2O_3, Act. I; Et_2O (*Fluka, puriss.*) was applied without further purification. ADM (*Fluka, purum*) was distilled before use. All azulenes except guaiazulene (**1a**; *Fluka, puriss.*) were synthesized according to literature procedures or were available from earlier work.

1.1. *[Rh^I(cod)(η^5-guaiazulene)]$^+BF_4^-$* (**3a**). [Rh^ICl(cod)]$_2$ (0.985 g, 2 mmol) [14], was dissolved in THF (40 ml) and treated with $AgBF_4$ (0.780 g, 4.0 mmol). The white precipitate of AgCl was filtered off over *Celite*. Guaiazulene (**1a**; 0.750 g, 3.8 mmol) in THF (10 ml) was added to the clear yellow filtrate. The yelow color disappeared immediately and the soln. became deep-red. After stirring for 0.5 h, Et_2O (20 ml) was added to the mixture. Complex **3a** formed a dark red, microcrystalline precipitate which was collected by filtration and washed with Et_2O (10 ml); yield, after drying in high vacuum: 1.71 g (91%, on the basis of added **1a**).

Data of **3a**. M.p. 229.7–230.2°. UV/VIS (CH_2Cl_2): λ_{max} 517.1 (3.73), 314.5 (4.26), 272.5 (4.26); λ_{min} 439.2 (3.54), 297.6 (4.19), 230.1 (4.19). IR ($CHCl_3$): 3030*m*, 1522*m*, 1476*w*, 1424*m*. ^1H-NMR ($CDCl_3$): 7.95 (*dd*, $^3J(6,5) = 10.86$, $^4J(6,8) = 1.68$, H–C(6)); 7.76 (*d*, $^4J(8.6) = 1.68$, H–C(8)); 7.71 (*d*, $^3J(5,6) = 10.86$, H–C(5)); 7.20 (*t*-like, $^3J(2,3) = 3.13$, $^2J(2,Rh) = 1.74$, H–C(2)); 6.25 (*d*; $^3J(3,2) = 3.13$, H–C(3)); 5.01 (br. *s*, olefin. H, cod); 4.34 (*m*, olefin. H, cod); 3.25 (*sept.*, $^3J = 6.88$, Me_2CH–C(7)); 2.54 (*s*, Me–C(4)); 2.23 (*s*, Me–C(1)); 2.04 (*m*, allyl. H, cod); 1.41 (2*d*, $J = 6.88$, Me_2CH–C(7)). ^1H-NOE ($CDCl_3$): 7.76 (H–C(8))→2.23 (*s*, Me–C(1)); 2.54 (Me–C(4))→7.71 (*s*, H–C(5)), 6.25 (*s*, H–C(1)), 4.94 (*w*, olefin. H, cod), and 4.34 (*m*, olefin. H, cod); 2.23 (*Me*–C(1))→7.76 (*s*, H–C(8)) and 7.20 (*s*, H–C(2)). ^1H-DR ($CDCl_3$): 6.25 (H–C(3))→7.20 (*d*, $^2J(2,Rh) = 1.74$, H–C(2)). ^{13}C-NMR ($CDCl_3$): 153.8 (*s*, C(4)); 145.3 (*s*, C(7)); 138.0 (*s*, C(5)); 136.3 (*s*, C(6)); 131.2 (*s*, C(8)); 111.9, 110.6 (*d*, $^1J(3a,Rh) = 3.9$, $^1J(8a,Rh) = 3.6$ or *vice versa*, C(3a,8a)); 106.0 (*d*, $^1J(2,Rh) = 5.0$, C(2)); 101.0 (*d*, $^1J(1,Rh) = 3.6$, C(1)); 84.8 (*d*, ^1J(olefin.C(cod),Rh) = 12.0, olefin. C(cod)); 84.4 (*d*, $^1J(3,Rh) = 4.1$, C(3)); 80.6 (*d*, ^1J(olefin.C(cod),Rh) = 11.2, olefin. C(cod)); 38.4 (*s*, Me_2CH–C(7)); 31.3, 29.4 (*s*, aliphat. C(cod)); 24.8, 24.5 (*s*, Me_2CH–C(7)); 23.8 (*s*, *Me*–C(4)); 10.6 (*s*, Me–C(1)). ^{103}Rh-NMR ($CDCl_3$): –44.5 (br. *d*; $\delta(^{103}Rh)$ relative to $\Xi(^{103}Rh) = 3.16$ MHz (*cf.* [10])). Anal. calc. for $C_{23}H_{30}BF_4Rh$ (496.21): C 55.67, H 6.09; found: C 55.85, H 5.89.

The structure of **3a** was confirmed by an X-ray structure analysis at $-100 \pm 1°$ (see *Fig. 1* for numbering). *Crystal data*[4]): monoclinic; space group $P2_1/c$; cell dimensions: $a = 11.689(4)$, $b = 10.771(6)$, $c = 17.148(6)$ Å, $\beta = 93.29(3)°$; $V = 2155(2)$ Å^3; $D_{calc} = 1.529$ Mg m^{-3}; $Z = 4$; $\mu(MoK_\alpha) = 8.181$ cm^{-1}; $2\theta_{max} = 60°$; 6895 measured, 6290 unique reflections; final $R = 0.0347$, $R_w = 0.0373$, $GoF = 2.277$ for 406 refined parameters and 5053 observed reflections [$I > 3\sigma(I)$]; $\Delta\rho$ (max, min) = 1.20, –0.61 e Å^{-3}. The intensities were collected on a *Rigaku AFC5R* rotating-anode diffractometer using graphite-monochromated MoK_α radiation ($\lambda = 0.71069$ Å) and $\omega/2\theta$ scan, and were corrected for *Lorentz* and polarization effects but not for absorption (ψ-scans showed that an absorption correction was unnecessary). The structure was solved by the *Patterson* method using SHELXS86 [15], which revealed the position of the Rh-atom. All remaining non-H-atoms were located in a *Fourier* expansion of the *Patterson* solution. The cod ring was disordered; two positions were defined for each atom of the ring, each

---

[4]) Atomic coordinates, bond lengths, and bond angles have been deposited with the *Cambridge Crystallographic Data Centre*, 12 Union Road, Cambridge, CB2 1EZ, England.

position being assigned a site occupation factor of 0.5. All non-H-atoms were refined anisotropically. All of the H-atoms, except those of the cod ring, were located in a difference electron-density map and were refined isotropically. The H-atoms of the cod ring were placed in geometrically calculated positions with fixed isotropic temp. factors. The BF_4^- anion was refined as an ordered group, although the thermal parameters of the F-atoms and a residual electron-density peak of 1.2 e $Å^{-3}$ in the final difference electron-density map indicated the possible presence of disorder. An attempt to refine a disordered model for the anion led to unsatisfactory results. The refinement was carried out on F using full-matrix least-squares procedures, which minimized the function $\Sigma\omega\,(|F_o| - |F_c|)^2$. Corrections for secondary extinction were not applied. All calculations were performed with the TEXSAN crystallographic software package [16]. Bond lengths and selected bond angles of **3a** are listed in *Table 4* and torsion angles for the cod ring of **3a** in *Table 5*.

All the other [$Rh^I(\eta^5$-azulene)(cod)$^+BF_4^-$ complexes **3b–g** were prepared by the procedure as described above, but on a smaller scale. [$Rh^ICl(cod)]_2$ (0.2 mmol), $AgBF_4$ (0.4 mmol), THF (5 ml), azulenes **1b–g** (0.35 mmol) (*cf.* [2] [17]) in THF (2 ml) and Et_2O (5 ml; *cf. Table 1*).

Table 4. *Bond Lengths* [pm] *and Selected Bond Angles* [°] *for* **3a**. E.s.d.'s in parentheses.

Rh–C(1)	227.1(3)	C(1)–C(2)	141.2(4)	C(16)–C(17)	137(1)
Rh–C(2)	228.3(3)	C(1)–C(10)	144.6(4)	C(16)–C(23)	152(1)
Rh–C(3)	221.6(3)	C(1)–C(11)	149.5(4)	C(17)–C(18)	153(1)
Rh–C(4)	227.8(3)	C(2)–C(3)	141.1(5)	C(18)–C(19)	153(1)
Rh–C(10)	226.6(3)	C(3)–C(4)	144.1(4)	C(19)–C(20)	151(1)
Rh–C(16)	220(1)	C(4)–C(5)	140.5(4)	C(20)–C(21)	149(4)
Rh–C(16A)	213.0(9)	C(4)–C(10)	147.0(4)	C(21)–C(22)	144(4)
Rh–C(17)	217(1)	C(5)–C(6)	140.0(4)	C(22)–C(23)	153(1)
Rh–C(17A)	216.5(9)	C(5)–C(12)	151.2(4)	C(16A)–C(17A)	136(1)
Rh–C(20)	220(2)	C(6)–C(7)	138.5(4)	C(16A)–C(23A)	148(1)
Rh–C(20A)	214(2)	C(7)–C(8)	140.8(4)	C(17A)–C(18A)	153(1)
Rh–C(21)	217(3)	C(8)–C(9)	138.5(4)	C(18A)–C(19A)	150(1)
Rh–C(21A)	218(3)	C(8)–C(13)	152.7(4)	C(19A)–C(20A)	154(1)
F(1)–B	135.4(4)	C(9)–C(10)	140.6(4)	C(20A)–C(21A)	127(4)
F(2)–B	138.0(4)	C(13)–C(14)	151.8(5)	C(21A)–C(22A)	158(4)
F(3)–B	138.8(4)	C(13)–C(15)	153.4(6)	C(22A)–C(23A)	150(1)
F(4)–B	136.1(4)				

C(2)–C(1)–C(10)	108.1(3)	C(8)–C(13)–C(14)	115.1(3)
C(2)–C(1)–C(11)	126.2(3)	C(8)–C(13)–C(15)	108.3(3)
C(10)–C(1)–C(11)	125.5(3)	C(14)–C(13)–C(15)	110.4(3)
C(1)–C(2)–C(3)	109.1(3)	C(17)–C(16)–C(23)	124.(1)
C(2)–C(3)–C(4)	109.0(3)	C(16)–C(17)–C(18)	126.(1)
C(3)–C(4)–C(5)	125.9(3)	C(17)–C(18)–C(19)	114.2(9)
C(3)–C(4)–C(10)	106.1(2)	C(18)–C(19)–C(20)	114.(1)
C(5)–C(4)–C(10)	127.8(3)	C(19)–C(20)–C(21)	124.(2)
C(4)–C(5)–C(6)	125.0(3)	C(20)–C(21)–C(22)	125.(2)
C(4)–C(5)–C(12)	117.6(3)	C(21)–C(22)–C(23)	114.(1)
C(6)–C(5)–C(12)	117.3(3)	C(16)–C(23)–C(22)	112.5(8)
C(5)–C(6)–C(7)	131.7(3)	C(17A)–C(16A)–C(23A)	125.(1)
C(6)–C(7)–C(8)	130.7(3)	C(16A)–C(17A)–C(18A)	123.3(9)
C(7)–C(8)–C(9)	125.1(3)	C(17A)–C(18A)–C(19A)	114.3(8)
C(7)–C(8)–C(13)	118.3(2)	C(18A)–C(19A)–C(20A)	114.(1)
C(9)–C(8)–C(13)	116.4(2)	C(19A)–C(20A)–C(21A)	124.(2)
C(8)–C(9)–C(10)	130.1(3)	C(20A)–C(21A)–C(22A)	128.(2)
C(1)–C(10)–C(4)	107.3(2)	C(21A)–C(22A)–C(23A)	114.(1)
C(1)–C(10)–C(9)	123.9(2)	C(16A)–C(23A)–C(22A)	115.8(9)
C(4)–C(10)–C(9)	128.6(2)		

Table 5. *Torsion Angles* [°] *for the cod ring of* **3a**

C(16)–C(17)–C(18)–C(19)	–42.(2)	C(16A)–C(17A)–C(18A)–C(19A)	–89.(1)
C(16)–C(23)–C(22)–C(21)	–35.(2)	C(16A)–C(23A)–C(22A)–C(21A)	22.(2)
C(17)–C(16)–C(23)–C(22)	97.(1)	C(17A)–C(16A)–C(23A)–C(22A)	52.(2)
C(17)–C(18)–C(19)–C(20)	–34.(2)	C(17A)–C(18A)–C(19A)–C(20A)	27.(1)
C(18)–C(17)–C(16)–C(23)	–5.(2)	C(18A)–C(17A)–C(16A)–C(23A)	0.(2)
C(18)–C(19)–C(20)–C(21)	89.(2)	C(18A)–C(19A)–C(20A)–C(21A)	53.(2)
C(19)–C(20)–C(21)–C(22)	2.(3)	C(19A)–C(20A)–C(21A)–C(22A)	–4.(4)
C(20)–C(21)–C(22)–C(23)	–45.(3)	C(20A)–C(21A)–C(22A)–C(23A)	–83.(3)

1.2. *[Rh^I(cod)(η^5-4,6,8-trimethylazulene)]$^+$BF$_4^-$* (**3b**). M.p. 190.8–192.1°. UV/VIS (CH_2Cl_2): λ_{max} 505.6 (3.78), 354.2 (sh, 3.93), 295.5 (4.26), 284.3 (4.27), 275 (br., 4.29), 248.6 (sh, 4.22); λ_{min} 421.2 (3.57), 392.4 (4.26), 381.1 (4.28); 254.2 (4.18). ^{1}H-NMR ($CDCl_3$): 7.67 (*s*, H–C(5,7)); 7.20 (*dd*, $^3J(2,1) = {}^3J(2,3) = 3.23$, $^2J(2,Rh) = 1.74$, H–C(2)); 6.23 (*d*, $^3J(1,2) = {}^3J(3,2) = 3.23$, H–C(1,3)); 4.70 (br. *s*, olefin. H, cod); 2.70 (*s*, Me–C(6)); 2.62 (*s*, Me–C(4,8)); 2.06–1.97 (*m*, allyl. H, cod). ^{13}C-NMR ($CDCl_3$): 153.2 (*s*, C(6)); 147.9 (*s*, C(4,8)); 136.5 (*s*, C(5,7)); 111.1 (*d*, ^1J(3a,Rh) = ^1J(8a,Rh) = 3.3, C(3a,8a)); 103.7 (*d*, $^1J(2,Rh) = 4.0$, C(2)); 88.2 (*d*, $^1J(1,Rh) = {}^1J(3,Rh) = 3.5$, C(1,3)); 80.2 (*d*, ^1J(olefin.C(cod),Rh) = 12.2, olefin. C(cod)); 30.6 (*s*, aliph. C(cod)); 29.3 (*s*, *Me*–C(6)); 25.6 (*s*, *Me*–C(4,8)). Anal. calc. for $C_{21}H_{26}BF_4Rh$ (468.15): C 53.88, H 5.60; found: C 53.95, H 5.75.

1.3. *[Rh^I(cod)(η^5-2,4,6,8-tetramethylazulene)]$^+$BF$_4^-$* (**3c**). M.p. 249.9–250.8°. UV/VIS (CH_2Cl_2): λ_{max} 508.2 3.83), 349.4 (sh, 3.75), 296.0 (sh, 4.23), 267.3 (4.36); λ_{min} 420.2 (3.54), 246.7 (4.24). ^{1}H-NMR ($CDCl_3$): 7.55 (*s*, H–C(5,7)); 6.22 (*s*, H–C(1,3)); 4.68 (br. *s*, olefin. H, cod); 2.74 (br. *s*, Me–C(2)); 2.64 (*s*, Me–C(6)); 2.57 (*s*, Me–C(4,8)); 2.01 (*s*, allyl. H, cod). ^{13}C-NMR ($CDCl_3$): 151.2 (*s*, C(6)); 146.2 (*s*, C(4,8)); 136.2 (*s*, C(5,7)); 110.8 (*d*, ^1J(3a,Rh) = ^1J(8a,Rh) = 3.3, C(3a,8a)); 108.4 (*d*, $^1J(2,Rh) = 4.8$, C(2)); 89.8 (*d*, $^1J(1,Rh) = {}^1J(3,Rh) = 3.3$, C(1,3)); 80.5 (*d*, ^1J(olefin.C(cod),Rh) = 12.2, olefin. C(cod)); 30.7 (*s*, aliph. C(cod)); 29.2 (*s*, *Me*–C(6)); 25.5 (*s*, *Me*–C(4,8)); 13.9 (*s*, *Me*–C(2)). Anal. calc. for $C_{22}H_{28}BF_4Rh$ (482.18): C 54.80, H 5.85; found: C 54.45, H 5.65.

1.4. *[Rh^I(cod){η^5(methyl 4,6-8-trimethylazulene-2-carboxylate)}]$^+$BF$_4^-$* (**3d**). M.p. 210.8–212.0°. UV/VIS (CH_2Cl_2): λ_{max} 532.2 (3.84), 367.1 (sh, 3.74), 303.7 (4.32), 291.3 (4.33); 270.1 (br., 4.34); 252.4 (4.30); λ_{min} 424.2 (3.52), 298.7 (4.30); 286.9 (4.33); 247.0 (4.28). ^{1}H-NMR ($CDCl_3$): 7.89 (*s*, H–C(5,7)); 6.43 (*s*, H–C(1,3)); 4.78 (br. *s*, olefin. H, cod); 4.09 (*s*, MeOCO–C(2)); 2.78 (*s*, Me–C(6)); 2.69 (*s*, Me–C(4,8)); 2.01 (br. *s*, allyl. H, cod). ^{13}C-NMR ($CDCl_3$): 163.2 (*s*, MeOCO–C(2)); 157.4 (*s*, C(6)); 150.6 (*s*, C(4,8)); 138.4 (*s*, C(5,7)); 112.9 (*d*, ^1J(3a,Rh) = ^1J(8a,Rh) = 2.8, C(3a,8a)); 104.8 (*d*, $^1J(2,Rh) = 3.8$, C(2)); 86.2 (*d*, $^1J(1,Rh) = {}^1J(3,RH) = 2.6$, C(1,3)); 81.8 (*d*, ^1J(olefin.C(cod),Rh) = 12.0, olefin. C(cod)); 53.1 (*s*, *Me*OCO–C(2)); 30.6 (*s*, aliph. C(cod)); 29.8 (*s*, *Me*–C(6)); 25.9 (*s*, *Me*–C(4,8)). Anal. calc. for $C_{23}H_{28}O_2BF_4Rh$ (526.19): C 52.50, H 5.36; found: C 52.31, H 5.65.

1.5. *[Rh^I(cod){η^5-6-(*tert*-*butyl*)-1,3-dimethylazulene}]$^+$BF$_4^-$* (**3e**)[5]. M.p. 179.8–180.6°. UV/VIS (CH_2Cl_2): λ_{max} 524.9 (3.77), 393.2 (sh, 3.67), 313.4 (4.29), 279.3 (br., 4.30); λ_{min} 432.1 (3.55), 300.7 (4.24); 253.0 (4.15). ^{1}H-NMR ($CDCl_3$): 7.97 (*AA'BB'* system, $^3J_{AB} = 10.8$, H–C(4,5,7,8)); 7.07 (*d*, $^2J(2,Rh) = 1.67$, H–C(2)); 4.55 (br. *s*, olefin.H, cod); 2.22 (*s*, Me–C(1,3)); 2.04 (br. *s*, allyl.H, cod), 1.49 (*s*, *t*-Bu). ^{13}C-NMR ($CDCl_3$): 164.9 (*s*, C(6)); 131.5, 130.9 (2*s*, C(4,8,5,7)); 108.8 (*d*, ^1J(3a,Rh) = ^1J(8a,Rh) = 3.9, C(3a,8a)); 107.7 (*d*, $^1J(2,Rh) = 4.7$, C(2)); 86.2 (*d*, $^1J(1,Rh) = {}^1J(3,Rh) = 3.9$, C(1,3)); 83.4 (*d*, ^1J(olefin.C(cod),Rh) = 12.0, olefin. C(cod)); 39.8 (*s*, Me_3C–C(6)); 31.0 (*s*, Me_3C–C(6)); 31.0 (*s*, aliph. C(cod)); 10.1 (*s*, Me–C(1,3)). Anal. calc. for $C_{24}H_{32}BF_4Rh$ (510.23): C 56.50, H 6.32; found: C 56.63, H 6.56.

1.6. *[Rh^I{η^5-6(*tert*-*butyl*)-1,3,4,8-tetramethylazulene(cod)}]$^+$BF$_4^-$* (**3f**). M.p. 200.9–201.8°. UV/VIS (CH_2Cl_2): λ_{max} 522.6 (3.82), 390.1 (sh, 3.69), 311.7 (4.27), 271.5 (4.35); λ_{min} 428.5 (3.56), 297.2 (4.24); 251.1 (4.22). ^{1}H-NMR ($CDCl_3$): 7.56 (*s*, H–C(5,7)); 7.93 (*d*, $^2J(2,Rh) = 1.24$, H–C(2)); 4.37 (br. *s*, olefin. H, cod); 2.69 (*s*, Me–C(4,8)); 2,37 (*s*, Me–C(1,3)); 2.22–2.09 (*m*, allyl. H, cod), 1.45 (*s*, *t*-Bu). ^{13}C-NMR ($CDCl_3$): 163.8 (*s*, C(6)); 147.9 (*s*, C(4,8)); 133.5 (*s*, C(5,7)); 113.9 (*d* and *s*, $^1J(2,Rh) = 4.1$, C(2,3a,8a)); 100.9 (*d*, $^1J(1,Rh) = {}^1J(3,Rh) = 3.0$, C(1,3)); 84.4 (*d*, ^1J(olefin.C(cod),Rh) = 11.9, olefin. C(cod)); 39.7 (*s*, Me_3C–C(6)); 30.9 (*s*, aliph. C(cod)); 30.8 (*s*, Me_3C–C(6)); 28.8 (*s*, *Me*–C(4,8)); 16.3 (*s*, Me–C(1,3)). Anal. calc. for $C_{26}H_{36}BF_4Rh$ (538.29): C 58.01, H 6.74; found: C 58.32, H 7.01.

1.7. *[Rh^I(cod)(η^5-1,2,3,4,6,8-hexamethylazulene)]$^+$BF$_4^-$* (**3g**). M.p. 210.5–211.6°. UV/VIS (CH_2Cl_2): λ_{max} 516.6 (3.82), 392.4 (sh, 3.61), 307.9 (4.23), 273.7 (4.31); λ_{min} 430.1 (3.35), 296.2 (4.20); 254.6 (4.21). ^{1}H-NMR

[5]) Azulene **1e** was prepared in the usual manner starting with 1-butyl-4-(*tert*-butyl)pyridinium bromide and sodium cyclopentadienide followed by formylation/reduction procedures (*cf.* [2] [18]); m.p. 67.5–68.2° [19].

($CDCl_3$): 7.39 (*s*, H–C(5,7)); 4.25 (br. *s*, olefin. H, cod); 2.68 (*s*, Me–C(4,8)); 2.54 (*s*, Me–C(6)); 2.53 (*d*, $^3J(Me–C(2),Rh) = 1.27$, Me–C(2)); 2.33 (*s*, Me–C(1,3)); 2.11 (br. *s*, allyl. H, cod). ^{13}C-NMR ($CDCl_3$): 150.8 (*s*, C(6)); 146.5 (*s*, C(4,8)); 137.2 (*s*, C(5,7)); 122.8 (*d*, $^1J(3a,Rh) = {}^1J(8a,Rh) \approx 4$, C(3a,8a)); 106.8 (*d*, $^1J(2,Rh) \approx 3$, C(2)); 101.3 (*d*, $^1J(1,Rh) = {}^1J(3,Rh) = 4.2$, C(1,3)); 84.1 (*d*, ^1J(olefin.C(cod),Rh) = 12.1, olefin. C(cod)); 30.8 (*s*, aliph. C(cod)); 28.7 (*s*, *Me*–C(4,8)); 28.2 (*s*, Me–C(6)); 13.8 (*s*, *Me*–C(1,3)); 11.6 (*s*, *Me*–C(2)). Anal. calc. for $C_{24}H_{32}BF_4Rh$ (510.23): C 56.50, H 6.32; found: C 56.84, H 6.58.

2. *Catalysis of Heptalene Formation.* 2.1. *Reaction of ADM with Complex* **3a**. In a closed *Schlenk* reaction vessel **3a** (0.100 g, 0.2 mmol) and ADM (0.025 ml, 0.2 mmol) were heated in MeCN (1 ml) at 100° under Ar during 18 h. The products were seperated on a small column of silica gel (hexane/Et_2O 3:2). In the order of elution were obtained *dimethyl (Z)-* and *(E)-1-(5-isopropyl-3,8-dimethylazulen-1-yl)ethene-1,2-dicarboxylate* ((*Z*)- and (*E*)-**4a**; 0.013 g, 19%, and 0.006 g, 9%, respectively) and *dimethyl 7-isopropyl-5,10-dimethylheptalene-1,2-dicarboxylate* (**2a**; 0.016 g, 23.5%).

2.2. *Reaction of Guaiazulene* (**1a**) *and ADM in the Presence of* **3a** *as a Catalyst.* In a closed *Schlenk* reaction vessel **1a** (0.198 g, 1.0 mmol), ADM (0.36 ml, 3.0 mmol), and **3a** (0.010 g, 0.02 mmol) were heated in MeCN (10 ml) at 100° under Ar during 18 h. Workup (*cf. 2.1*) gave (*Z*)-**4a** (0.018 g, 5.3%), (*E*)-**4a** (0.010 g, 2.9%), and **2a** (0.280 g, 82.4%).

2.3. *Reaction of Guaiazulene* (**1a**) *and ADM in the Presence of* in situ *Generated* **3a**. In a closed *Schlenk* reaction vessel **1a** (0.198 g, 1.0 mmol), ADM (0.36 ml, 3.0 mmol), $[Rh^I(cod(Cl)]_2$ (0.005 g, 0.01 mmol), and $AgBF_4$ (0.004 g, 0.02 mmol) were heated in MeCN (10 ml) at 100° under Ar during 18 h. Workup (*cf. 2.1*) gave (*Z*)-**4a**(0.022 g, 6.4%), (*E*)-**4a** (0.009 g, 2.7%), and **2a** (0.273 g, 80.2%).

2.4. *Reaction of Guaiazulene* **1a** *and ADM in the Presence of* $[Rh^ICl(cod)]_2$ *as a Catalyst.* In a closed *Schlenk* reaction vessel **1a** (0.198 g, 1.0 mmol), ADM 0.36 ml, 3.0 mmol), and $[Rh^ICl(cod)]_2$ (0.005 g, 0.01 mmol) were heated in MeCN (10 ml) at 100° under Ar during 18 h. Workup (*cf. 2.1*) gave (*Z*)-**4a** (0.018 g, 5.3%), (*E*)-**4a** (0.013 g, 3.8%), and **2a** (0.269 g, 79.1%).

2.5. *Reaction of Guaiazulene* (**1a**) *and ADM in the Presence of* $[Rh^IH(PPh_3)_4]$ *as a Catalyst.* In a closed *Schlenk* reaction vessel **1a** (0.198 g, 1.0 mmol), ADM (0.36 ml, 3.0 mmol), and $[Rh^IH(PPh_3)_4]$ (0.022 g, 0.02 mmol) [20] were heated in MeCN (10 ml) at 100° under Ar during 18 h. Workup (*cf. 2.1*) gave (*Z*)-**4a** (0.036 g, 10.6%), (*E*)-**4a** (0.021 g, 6.2%), and **2a** (0.221 g, 65.0%).

REFERENCE

[1] A. J. Rippert, H.-J. Hansen, *Helv. Chim. Acta* **1991,** *75,* 2219.
[2] Y. Chen, R. W. Kunz, P. Uebelhart, R. H. Weber, H.-J. Hansen, *Helv. Chim. Acta* **1992,** *75,* 2447.
[3] R. H. Fallahpour, H.-J. Hansen, *High Pressure Res.* **1992,** *11,* 125.
[4] R. R. Schrock, J. A. Osborn, *J. Am. Chem. Soc.* **1971,** *93,* 3089.
[5] G. Bombieri, G. Tresoldi, F. Faraone, G. Bruno, P. Cavoli-Belluco, *Inorg. Chim. Acta* **1982,** *57,* 1.
[6] G. Moran, M. Green, A. G. Orpen, *J. Organomet. Chem.* **1983,** *250,* C15.
[7] J. W. Park, P. B. Mackenzie, W. P. Schaefer, R. H. Grubbs, *J. Am. Chem. Soc.* **1986,** *108,* 6402.
[8] M. J. Chetcuti, J. A. K. Howard, M. Pfeffer, J. L. Spencer, F. G. A. Stone, *J. Chem. Soc., Dalton Trans.* **1981,** 276.
[9] W. J. Hälg, L. R. Oehrström, H. Rüegger, L. M. Venanzi, T. Gerfin, V. Gramlich, *Helv. Chim. Acta* **1993,** *76,* 788; see also W. J. Hälg, L. R. Oehrström, H. Rüegger, L. M. Venanzi, *Magn. Res. Chem.* **1993,** *31,* 677.
[10] a) R. Garth, R. J. Goodfellow, in 'NMR and the Periodic Table', Eds. R. K. Harris, B. E. Mann, Acedemic Press, Inc., New York 1978, p. 248ff. b) R. J. Goodfellow, in 'Multinuclear NMR', Ed. J. Mason, Plenum Press, New York, 1987, p. 521ff.
[11] T. Mitsudo, Y. Hori, Y. Watanabe, *J. Organomet. Chem.* **1987,** *334,* 157.
[12] W. Treibs, *Naturwiss.* **1965,** *52,* 452.
[13] K. Hafner, H. Diehl, H. V. Süss, *Angew. Chem.* **1976,** *88,* 121; *ibid. Int. Ed.* **1976,** *15,* 104.
[14] G. Giordano, R. H. Crabtree, *Inorg. Synth.* **1990,** *28,* 83.
[15] G. M. Sheldrick, SHELXS86, *Acta Crystallogr., Sect. A* **1990,** *46,* 467.
[16] TEXSAN-TEXRAY Single Crystal Structure Analysis Package, Version 5.0 Molecular Structure Corporation, The Woodlands, Texas, 1989.
[17] K. Hafner, H. Kaiser, *Org. Synth., Coll. Vol.* **1973,** *5,* 1088.
[18] R. H. Alder, G. Whittacker, *J. Chem. Soc., Perkin Trans. 2* **1975,** 714.
[19] P. Uebelhart, H.-J. Hansen, unpublished result.
[20] N. Ahmad, J. J. Levion, S. D. Robinson, M. F. Uttley, *Inorg. Synth.* **1990,** *28,* 81.